Open-PMC-18M: A High-Fidelity Large Scale Medical Dataset for Multimodal Representation Learning

Anonymous Author(s)
Affiliation
Address
email

Abstract

Compound figures, which are multi-panel composites containing diverse subfigures, are ubiquitous in biomedical literature, yet large-scale subfigure extraction remains largely unaddressed. Prior work on subfigure extraction has been limited in both dataset size and generalizability, leaving a critical open question: *How does high-fidelity image–text alignment via large-scale subfigure extraction impact representation learning in vision-language models?* We address this gap by introducing a scalable subfigure extraction pipeline based on transformer-based object detection, trained on a synthetic corpus of 500,000 compound figures, and achieving state-of-the-art performance on both ImageCLEF 2016 and synthetic benchmarks. Using this pipeline, we release **OPEN-PMC-18M**, a large-scale high quality biomedical vision-language dataset comprising *18 million* clinically relevant subfigure–caption pairs spanning radiology, microscopy, and visible light photography. We train and evaluate vision-language models on our curated datasets and show improved performance across retrieval, zero-shot classification, and robustness benchmarks, outperforming existing baselines. We release our dataset, models, and code to support reproducible benchmarks and further study into biomedical vision-language modeling and representation learning.

1 Introduction

The rapid progress of general-domain vision-language models (VLM) (Radford et al., 2021; Jia et al., 2021; Girdhar et al., 2023) has sparked growing interest in building large-scale multimodal datasets tailored to the medical domain (Zhang et al., 2023; Lin et al., 2023a; Pelka et al., 2018; Lozano et al., 2025; Baghbanzadeh et al., 2025). Despite these efforts, the scale of medical datasets still lags far behind their general-domain counterparts. While increasing dataset *size* continues to be a primary goal, there is growing recognition that improving the *quality* and *relevance* of image-text pairs may be a more effective strategy for enhancing model performance and clinical utility (Baghbanzadeh et al., 2025).

Biomedical figures present unique challenges: they often consist of compound layouts that combine multiple subfigures, each potentially depicting a different imaging modality, anatomical region, or clinical concept. Unlike dataset scale, which has received substantial attention, this structural heterogeneity remains largely unexplored. Most of the existing biomedical VLM pipelines treat compound figures as atomic units, pairing the entire image with a caption, without disentangling their internal structure.

We hypothesize that such coarse image-text alignment could introduce noise into pretraining, ultimately impacting the transferability and generalizability of the learned representations. While recent

Submitted to 39th Conference on Neural Information Processing Systems (NeurIPS 2025). Do not distribute.

work has scaled data curation through bulk mining of PubMed Central (PMC)[1] articles (e.g., PMC-15M (Zhang et al., 2023) and BIOMEDICA (Lozano et al., 2025)), these efforts still rely on noisy and compound figures. To our knowledge, only a few prior works incorporate subfigure extraction as part of the curation process (Pelka et al., 2018; Lin et al., 2023a; Baghbanzadeh et al., 2025); however, they do so at small scale. This raises an important gap in the field: *how does subfigure extraction and the resulting improvement in medical image-text alignment quality impact representation learning at scale, particularly given the known sensitivity of contrastive objectives to both dataset size and alignment fidelity during pretraining?*

In this work, we investigate the impact of large-scale subfigure extraction on medical vision-language representation learning. We first create a dataset of 6 million image-caption pairs by filtering out non-medical images (e.g., charts, plots, tables) from the BIOMEDICA corpus (Lozano et al., 2025) using a combination of label metadata and a ResNet classifier. For the *subfigure extraction* step, we train a high-performance object detection model with the same architecture as DAB-DETR (Dynamic Anchor Boxes DEtection TRansformer) (Liu et al., 2022) on a corpus of 500,000 programmatically-created compound figures. By decomposing compound figures with this model, we build OPEN-PMC-18M, one of the largest and most curated collections of biomedical image-text pairs to date, consisting of 18 million subfigure-caption pairs. We then train vision and text encoders using a contrastive learning objective and evaluate the resulting models on an extensive suite of downstream tasks, including cross-modal retrieval and zero-shot classification across three distinct medical modalities: radiology, microscopy, and visible light photography (VLP). We release our dataset[2], models, and code[3] to support reproducible benchmarks and further study into biomedical VLM and representation learning. Our contributions are as follows:

- We propose a scalable subfigure extraction pipeline using transformer-based object detection trained on a 500,000 compound figure dataset, achieving state-of-the-art performance on ImageCLEF 2016 (Kalpathy-Cramer et al., 2014; García Seco de Herrera et al., 2016) and synthetic evaluation sets.
- We release OPEN-PMC-18M, a large-scale biomedical image-text dataset with 18 million subfigure-caption pairs filtered for clinical relevance across radiology, microscopy, and visible light photography.
- We provide a comprehensive evaluation of vision-language models trained on our datasets, demonstrating improved performance in retrieval, classification, and robustness across multiple medical benchmarks.

2 Related Work

2.1 Biomedical Vision-Language Datasets

Most efforts to date have relied on mining figures and captions from the PMC Open Access subset.[4] One of the earliest publicly available datasets is ROCO (Pelka et al., 2018), which compiled around 80,000 radiology and 6,000 non-radiology images, enriched with metadata such as captions and keywords. Later, Lin et al. (2023b) introduced PMC-OA , which includes 1.6 million image-text pairs. Their contribution emphasized automation—proposing a pipeline to streamline the pairing process and reduce human annotation. More recently, Zhang et al. (2023) announced PMC-15M, a dataset of 15 million image-text pairs. The largest released dataset to date is BIOMEDICA (Lozano et al., 2025), which comprises 24 million pairs and employs clustering, vision encoders, and expert taxonomies to assign modality labels at global and local levels. While these efforts represent major progress in scale, recent work has emphasized that data quality is a critical factor in learning effective and generalizable medical representations (Baghbanzadeh et al., 2025). Building on the premise of OPEN-PMC, our work takes a quality-first approach while also significantly scaling up the dataset.

[1] https://pmc.ncbi.nlm.nih.gov/

[2] https://huggingface.co/datasets/vector-institute/open-pmc-18m

[3] https://anonymous.4open.science/r/open-pmc-18m-CE25/

[4] https://pmc.ncbi.nlm.nih.gov/tools/openftlist/

2.2 Subfigure Extraction as Object Detection

Early approaches to compound figure separation relied on classical computer vision techniques, using heuristics based on whitespace, edge detection, or layout regularity. However, these methods often struggled to handle diverse panel styles and complex spatial arrangements. More recent work treats subfigure extraction as an object detection problem, leveraging deep learning models. For example, Tsutsui and Crandall (2017) and Yao et al. (2021) used YOLO for subfigure separation. Lin et al. (2023a) also uses an object detection model to extract subfigures in their pipeline. They train a DETR (DEtection TRansformer) (Carion et al., 2020) model on the MedICaT dataset (Subramanian et al., 2020) containing 2069 annotated compound figures.

Data annotation for training an image decomposition model is challenging and time-consuming. Current annotated datasets for this are small, which lead to models with suboptimal performance. To overcome this, synthetic datasets of compound figures have been proposed, where subfigures are programmatically composed to simulate real-world layouts. This allows training of object detection models without relying on large-scale human-annotated data (Tsutsui and Crandall, 2017; Yao et al., 2021).

3 Data Composition and Curation Process

3.1 Initial Collection and Filtering

We begin with the BIOMEDICA dataset (Lozano et al., 2025), which has been extracted from articles in the PubMed Central Open Access Subset. BIOMEDICA contains approximately 24 million image-caption pairs along with metadata, including global and local modality labels for each image. We apply a filtering step using the provided labels and retain only those pairs primarily categorized as clinical imaging, microscopy, immunoassays, or chemical structure. This yields a dataset of 6 million pairs, which we refer to as PMC-6M in this paper.

3.2 Vision-Based Subfigure Extraction

To enable scalable extraction of subfigures from biomedical compound figures, we trained a transformer-based object detection architecture, Dynamic Anchor Box DEtection TRansformer (DAB-DETR) (Liu et al., 2022). Prior work of Lin et al. (2023a) trained a DETR model on MedICaT (Subramanian et al., 2020) with only 2,069 manually annotated compound figures. In contrast, we trained our model on a large-scale synthetic dataset of 500,000 compound figures, the first of its kind in the biomedical domain. We use DAB-DETR as it improves upon the original DETR model by learning dynamic anchors as queries, resulting in improved localization and faster convergence (Liu et al., 2022).

Synthetic Data Formation. To train a subfigure extraction model at scale, we generate a synthetic dataset by reversing the subfigure extraction process: rather than decomposing existing compound figures, we programmatically construct new ones by composing multiple single-panel biomedical images into compound layouts. The key advantage of this approach is the availability of ground-truth bounding boxes for each subfigure. Our generation pipeline samples a layout template that specifies the spatial arrangement of subfigures. Each layout is defined by a set of configurable parameters, including:

- **Grid Size**: Specifies a standard $m \times n$ grid or a custom arrangement for panel placement.
- **Margins**: Random horizontal and vertical spacing between panels to simulate variability in published figure layouts.
- **Labeling Scheme**: Determines how panels are annotated (e.g., using numerical, alphabetical, or compound labels like "1a" or "a-1"), and whether labels appear inside or outside panel boundaries.
- **Aspect Ratio**: Specifies a fixed width-to-height ratio applied uniformly to all subfigures.

Subfigures are sampled from a repository of single-panel biomedical images spanning diverse modalities such as radiology, microscopy, pathology, etc., which we will describe below. Composite figures may contain panels from the same modality or a heterogeneous mix, providing semantic

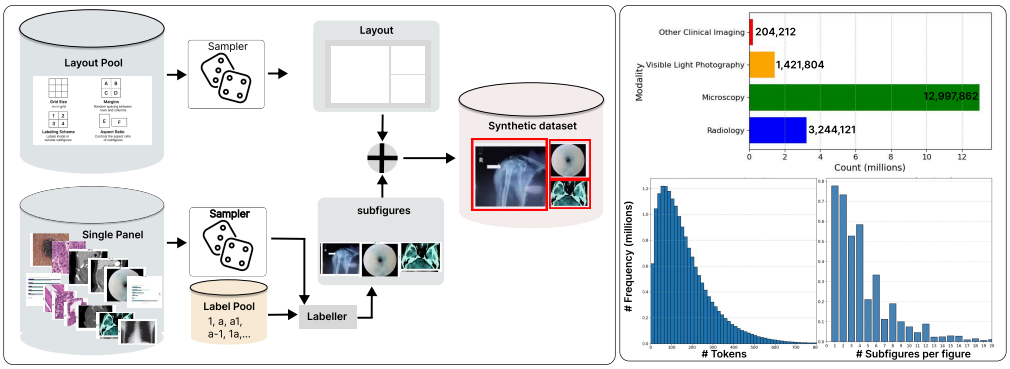

Figure 1: **Left** Overview of our pipeline for creating synthetic compound figures used to train the DAB-DETR model. A *Sampler* selects single-panel images and layout specifications from their respective pools. A *Labeler* assigns subfigure labels from a predefined label pool (e.g., 1, a, a1, a-1), placing them according to the chosen scheme. **Right** Distribution of medical image modalities, number of subfigures per compound figure, and caption length statistics within OPEN-PMC-18M. The average caption contains 165.82 tokens, with a max of 7352 and almost 19.48% of captions had more than 256 tokens.

diversity and mimicking real-world figure complexity. Figure 2) illustrates the full synthetic data pipeline.

Image Decomposition Model Training and Evaluation. We train a DAB-DETR model on the 500,000 synthetic compound figures and validate its performance on a similarly created holdout set of 20,000 images. Source subfigures are drawn from well-known benchmark datasets such as ROCO (Pelka et al., 2018), SICAP (Ángel E. Esteban et al., 2019), HAM10000 (Tschandl et al., 2018), PathMNIST and RetinaMNIST from MedMNIST (Yang et al., 2021, 2023), PAD-UFES-20 (Pacheco et al., 2020), and PlotQA (Methani et al., 2020) as listed in Table 1. To ensure balanced representation, each modality-specific dataset contributes approximately 16.7% of the total examples, with the remaining 16.7% comprising mixed-modality compound figures. This configuration promotes both visual diversity and generalization across biomedical imaging types. Training is performed over 40 epochs using a batch size of 64 and an initial learning rate of 1e-5. We evaluate performance on both our synthetic validation set and the ImageCLEF 2016 compound figure separation benchmark (Kalpathy-Cramer et al., 2014; García Seco de Herrera et al., 2016). Our model outperforms the model trained on MedICaT only on both evaluation sets as shown by Table 2. Figure 2 showcases examples from the ImageCLEF 2016 dataset and from a subset of PMC-6M, illustrating accurate detection of distinct subfigures across diverse panel layouts and content types.

Table 1: Datasets used for synthetic subfigure generation, categorized by modality and split.

Split	**Radiology**	**Histopathology**	**Dermatology**	**Retina**	**Plots**
Train	ROCO	SICAP	HAM10000	RetinaMNIST	PlotQA
Sample Size	65422	18783	10015	1080	60000
Validation	ROCO (test)	PathMNIST	PAD-UFES-20	RetinaMNIST (val)	PlotQA (val)
Sample Size	8176	10004	2298	120	10000

Table 2: Performance comparison on two datasets using mAP and F1 metrics.

Model	**Synthetic Validation**		**ImageCLEF 2016**	
	mAP (%)	**F1 (%)**	**mAP (%)**	**F1 (%)**
Previous model (MedICaT)	33.22	73.18	28.20	64.85
Our model (DAB-DETR)	**98.58**	**99.96**	**36.88**	**73.55**

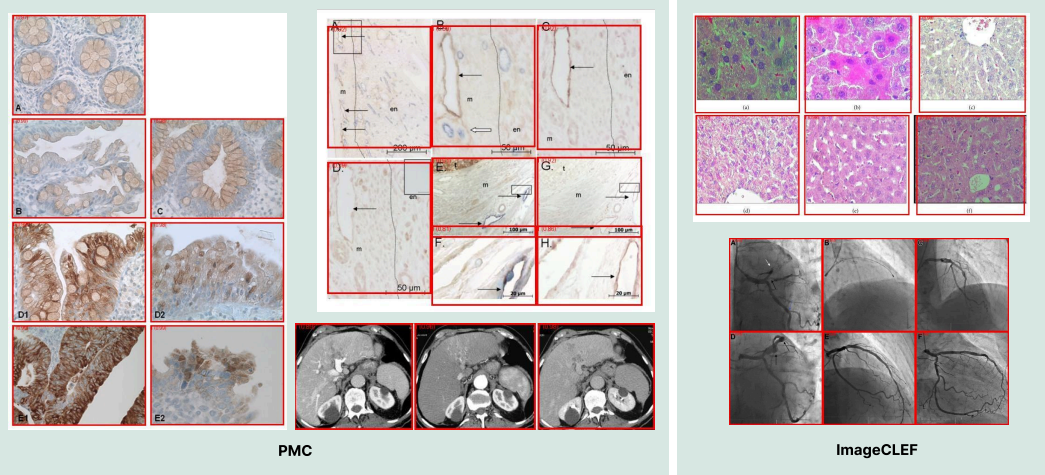

Figure 2: Qualitative results of subfigure detection using our DAB-DETR model. **Left** Real-world biomedical compound figures from PMC articles in PMC-6M (also BIOMEDICA). **Right** Examples from the ImageCLEF 2016 benchmark. The model accurately localizes and separates distinct subfigures, including heterogeneous panels and non-uniform layouts.

3.3 Curating OPEN-PMC-18M

Decomposing the compound images of PMC-6M using our DAB-DETR model yields an initial dataset of approximately 32 million single-panel images representing a wide range of clinical (e.g., radiology, pathology, microarray) and non-clinical (e.g., plots) images. For each figure, we simply pair the caption of the source compound figure to create the image-caption pair.

Filtering Pipeline To further refine the raw collection of 32 million image-caption pairs, we apply an additional layer of filtering by reviewing metadata fields to only keep subfigures whose original compound figure was labeled by either Clinical Image or Microscopy, which yields a dataset of 26 million pairs. Subsequently, we employ a ResNet-101 model (Lin et al., 2023a) to assess each image and infer its medical relevance. This filtering process further reduces the dataset to 18 million high-quality image-caption pairs.

Dataset Statistics We summarize the key characteristics of OPEN-PMC-18M below:

- **Image Modalities:** The dataset includes subfigures from three primary biomedical image modalities, as illustrated in Figure 1: radiology scans (e.g., CT, MRI, X-ray) comprising 18% of the dataset, pathology and microscopy images accounting for 73%, and visible light photography (VLP) representing 8%.
- **Caption Length:** Captions vary in length and complexity. The average caption contains 165.8 tokens. The maximum length is 7352 and almost 19.48% of captions have more than 256 tokens.

4 Experiments

4.1 Encoder Pretraining

As a first step, we train separate encoders for image and text modalities by aligning their representations using a vanilla contrastive loss. Let φ denote an image encoder and ψ denote a text encoder that maps images and text to a common representation space, respectively. Given a batch of training samples $B = \{(x_i, t_i)\}_{i=1}^{N}$, where x_i and t_i denote the i^{th} image and text instances respectively, the InfoNCE loss (Oord et al., 2018) is optimized by minimizing the distance between the representations of an image and its corresponding text, $(\varphi(x_i), \psi(t_i))$, while maximizing the distance between

unrelated image-text representation pairs, $(\varphi(x_i), \psi(t_j)),\ i \neq j$:

$$\ell_{\text{con}}(x_i, t_i; B) = -\left(\log \frac{\exp(\langle \varphi(x_i), \psi(t_i) \rangle / \tau)}{\sum_{k=1}^{N} \exp(\langle \varphi(x_i), \psi(\boldsymbol{t_k}) \rangle / \tau)} + \log \frac{\exp(\langle \varphi(x_i), \psi(t_i) \rangle / \tau)}{\sum_{k=1}^{N} \exp(\langle \varphi(\boldsymbol{x_k}), \psi(t_i) \rangle / \tau)}\right), \quad (1)$$

where $\langle \cdot, \cdot \rangle$ denotes similarity between two vectors (e.g. cosine similarity), and $\tau > 0$ is a temperature parameter. For simplicity of notation, we drop B and denote the loss for (x, t) by $\ell_{\text{con}}(x, t)$. Multimodal contrastive learning trains encoders φ and ψ by minimizing Eq. 1 over the pairs in B:

$$\ell_{\text{multimodal}} = \min_{\varphi, \psi} \ \mathbb{E}_B \Big[\frac{1}{N} \sum_{i=1}^{N} \ell_{\text{con}}(x_i, t_i)\Big]. \quad (2)$$

4.2 Evaluation Setup

To systematically assess the impact of dataset scale and curation quality, we perform evaluations along both dimensions. Our models are trained under a unified architecture and training protocol to ensure controlled evaluation. For models without accessible training data, we instead use publicly released checkpoints obtained from HuggingFace. For the text encoder, we use PubMedBERT (Gu et al., 2020), and for the vision encoder, we adopt a ViT-B/16 transformer (Dosovitskiy et al., 2020) pretrained on ImageNet. The encoders are trained for 64 epochs with batch size of 2048. The best-performing checkpoints for each encoder are selected based on validation retrieval performance. The training was performed using 8 NVIDIA A100 GPUs and completed in five days. We conducted our experiments using the mmlearn multimodal learning framework, available at https://github.com/VectorInstitute/mmlearn/tree/main.

For assessing the role of quality, particularly subfigure-level extraction, we train a baseline model on the 6 million compound figure-caption pairs of PMC-6M, where each compound image is used in its original form without panel separation (section 3.2). We also include publicly available checkpoints from other models trained on PMC-15M (Zhang et al., 2023) and BIOMEDICA (Lozano et al., 2025). For BIOMEDICA, we use the checkpoint referred to as $\texttt{BMC-CLIP}_{\text{CF}}$ in Lozano et al. (2025), which is trained on a filtered subset of the full dataset. This subset retains content labeled under clinical and scientific imaging, immunoassays, illustrative diagrams, chemical structures, maps, tools and materials, and hand-drawn or screen-based visuals, while explicitly excluding tables and charts. The model is trained for 36 epochs. For PMC-15M, we use the checkpoint trained on 15 million image-caption pairs, referred to as `BioMedCLIP` in Zhang et al. (2023). All external checkpoints were obtained from their official HuggingFace repositories and are evaluated using our standardized downstream protocols.

To further ensure consistency, we independently reproduce the PMC-OA dataset (Lin et al., 2023b) and train encoders using the same architecture and hyperparameters as those used for OPEN-PMC-18M and PMC-6M. Throughout the paper, all encoder variants are referenced by the name of the dataset on which they are trained, to facilitate transparent comparison. All the details of pretraining and hyperparameters are listed in the supplementary material.

4.3 Downstream Tasks

The performance of the encoders is evaluated on external and non-PMC datasets across two primary tasks: retrieval and zero-shot classification. For the retrieval task, we assess both image-to-text (I2T) and text-to-image (T2I) retrieval across three benchmark datasets representative of distinct medical imaging modalities: Quilt (Ikezogwo et al., 2024) (microscopy), MIMIC-CXR (Johnson et al., 2019) (radiology), and DeepEyeNet (Huang et al., 2021) (VLP). To evaluate robustness in retrieval, we follow established protocols from Liu et al. (2024) by applying a suite of low-level visual perturbations, including brightness adjustment, spatial shift, rotation, horizontal flip, and zoom, directly to the test images. To assess the statistical significance of robustness differences, we employ the Wilcoxon signed-rank test, a non-parametric method for paired comparisons (Wilcoxon, 1945). We consider a p-value less than 0.01 as statistically significant. For classification, we evaluate models using both zero-shot and linear probing protocols across a diverse set of tasks: five in radiology, eight in microscopy, and six in VLP. We use our trained vision and text encoders to encode the image and question, respectively.

4.4 Cross-Modal Retrieval and Robustness

Table 3 summarizes the performance of various VLMs on cross-modal retrieval tasks across three benchmark datasets: MIMIC-CXR, Quilt, and DeepEyeNet. We report Recall@200 (other Recall metrics are listed in the supplementary material) for both image-to-text and text-to-image retrieval, with the final column showing the Average Recall (AR) aggregated across all tasks. Models trained on OPEN-PMC-18M and even PMC-6M (compound figures) consistently outperform PMC-15M and BIOMEDICA, across all three tasks and retrieval directions. Among them, PMC-6M achieves the highest AR of 21.22, while OPEN-PMC-18M sets a new state-of-the-art with an AR of 21.64. This represents 31% relative gain in average retrieval performance over PMC-15M.

Robustness, quantified as the ratio between retrieval performance under perturbations (explained in section 4.2) and performance on the original data is presented in Figure 3 (Right). Models trained on OPEN-PMC-18M consistently achieve higher robustness scores relative to baseline models, reflecting improved performance stability under input perturbations in addition to superior retrieval performances. We observe statistically significant differences ($p < 0.01$) on Quilt and DeepEyeNet as shown in Figure 3 (Left). These findings are particularly relevant to our focus on subfigure extraction and the potential for improved robustness in imaging modalities that exhibit high visual and semantic heterogeneity.

Table 3: Retrieval performance (Recall@200) of all models trained on paired image-caption pairs in the medical domain. The last column, Average Recall (AR), aggregates the results across all tasks. Highest performance values are in bold, second-best are underlined. PMC-6M refers to a baseline model trained on a filtered subset of the BIOMEDICA dataset, using compound figures in their original form without subfigure decomposition. The BIOMEDICA model retrieved from Hugging Face is trained on a filtered subset of the full dataset, as described in their original paper.

	Image-to-Text			Text-to-Image			
Model	**MIMIC**	**Quilt**	**DeepEyeNet**	**MIMIC**	**Quilt**	**DeepEyeNet**	**AR**
PMC-OA	0.139	0.142	0.152	0.152	0.149	0.157	0.148
OPEN-PMC	0.17	0.166	0.183	0.189	0.162	0.147	0.17
BioMedCLIP	0.185	0.165	0.162	0.162	0.185	0.146	0.167
BIOMEDICA	0.076	0.169	0.155	0.093	0.195	0.145	0.139
PMC-6M	**0.25**	<u>0.203</u>	<u>0.172</u>	**0.257**	<u>0.22</u>	<u>0.170</u>	<u>0.212</u>
OPEN-PMC-18M	<u>0.226</u>	**0.211**	**0.196**	<u>0.239</u>	**0.233**	**0.193**	**0.216**

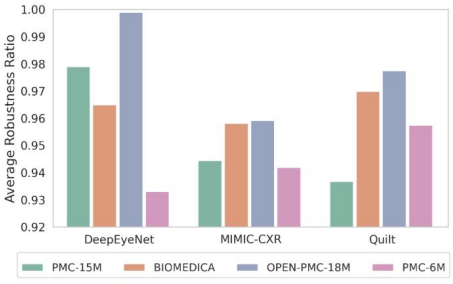

Model	**PMC-6M**	**BIOMEDICA**	**PMC-15M**
DeepEyeNet	0.0014	0.0073	$p > 0.01$
Quilt	0.0032	$p > 0.01$	0.0001
MIMIC-CXR	$p > 0.01$	$p > 0.01$	$p > 0.01$

Figure 3: **Left** Average robustness ratio across three retrieval benchmarks, defined as the ratio of retrieval performance under visual perturbations to that on original (unperturbed) data. **Right** Paired statistical comparisons (Wilcoxon signed-rank test) between OPEN-PMC-18M and each baseline model. Results show statistically significant improvements ($p < 0.01$) on DeepEyeNet and Quilt for at least one baseline comparison, while differences on MIMIC-CXR are not statistically significant across any of the baselines.

4.5 Zero-shot Classification

Model comparisons for zero-shot classification are presented in Table 4, and linear probing results are provided in the supplementary material. Results are grouped and averaged by modality. Models trained on OPEN-PMC-18M consistently achieve the highest average performance across modalities,

demonstrating superior transferability relative to all other evaluated models. Across the full set of 18 classification tasks spanning radiology, microscopy, and VLP , OPEN-PMC-18M ranks first in 6 tasks and second in 2. A similar trend is observed in the linear probing results, where OPEN-PMC-18M also achieves the highest average performance across modalities.

Table 4: Zero-shot classification F1-scores across diverse medical datasets for different models. For details on model training configurations and dataset sources, refer to the retrieval results table and its caption (Table 3).

	Radiology					
Model	**PneumoniaMNIST+**	**BreastMNIST+**	**OrganAMNIST+**	**OrganCMNIST+**	**OrganSMNIST+**	Average
PMC-OA	50.94	52.36	19.70	14.79	16.99	30.95
OPEN-PMC	50.13	**59.65**	**27.95**	**23.23**	**20.03**	36.19
BioMedCLIP	60.13	33.76	19.40	14.12	16.00	28.62
BIOMEDICA	38.46	**56.66**	19.25	17.13	16.33	29.56
PMC-6M	68.81	26.87	23.48	14.68	17.57	30.28
OPEN-PMC-18M	**86.18**	50.36	18.75	14.33	13.65	**36.65**

	Visible Light Photography						
Model	**PAD-UFES-20**	**Skin Cancer**	**PathMNIST+**	**DermaMNIST+**	**OCTMNIST+**	**RetinaMNIST+**	Average
PMC-OA	17.18	13.30	56.03	14.29	**50.74**	**27.22**	29.79
OPEN-PMC	21.11	13.56	49.16	14.60	45.27	26.12	28.30
BioMedCLIP	24.41	13.62	42.27	14.07	11.87	20.82	21.17
BIOMEDICA	**40.57**	17.20	49.10	**21.89**	10.00	18.53	26.21
PMC-6M	33.04	16.56	52.17	17.52	46.91	22.81	31.50
OPEN-PMC-18M	24.38	**18.28**	**60.75**	17.01	46.28	23.15	**31.64**

	Microscopy								
Model	**Sicap**	**PCam**	**NCT-CRC-HE**	**LC-Lung**	**LC-Colon**	**BACH**	**BloodMNIST+**	**TissueMNIST+**	Average
PMC-OA	32.80	70.65	43.95	56.04	**91.05**	33.75	5.57	**7.17**	42.62
OPEN-PMC	20.71	38.96	42.88	63.97	88.38	41.31	10.73	6.08	39.12
BIOMEDICA	31.80	62.17	48.98	70.93	84.43	39.83	4.37	4.31	43.35
BioMedCLIP	**41.53**	**72.57**	49.46	76.63	86.54	23.88	6.83	3.86	45.16
PMC-6M	22.89	68.05	55.28	**86.86**	78.41	52.58	3.72	3.05	46.35
OPEN-PMC-18M	16.29	69.55	**64.42**	86.01	71.94	**67.94**	**28.42**	3.74	**51.03**

4.6 Representations Analysis

To explore differences in the structure of learned image representations, we project the embedding spaces of three benchmark sets, each constructed by combining datasets used for retrieval and zero-shot classification across radiology, microscopy, and visible light photography (VLP), into two dimensions using t-SNE (Figure 4). The radiology benchmark includes MIMIC-CXR and other related zero-shot classification tasks, totaling approximately 41,000 samples. The microscopy and VLP benchmarks contain approximately 20,000 and 6,000 samples, respectively. To quantify differences between the embedding distributions, we compute the Maximum Mean Discrepancy (MMD) Gretton et al. (2012). Given a dataset X (e.g., all radiology samples), we extract embeddings $\phi(X)$ and $\psi(X)$ using vision encoders ϕ and ψ trained on OPEN-PMC-18M and PMC-6M, respectively. To assess whether the differences between these distributions are statistically significant, we perform a permutation test by randomly reassigning samples and recomputing MMD over 100 iterations to generate an empirical null distribution.

Visual inspection of the embeddings reveals distinct representational structures between the two models. This distinction is particularly evident in microscopy and VLP, where the latent spaces of the two models are more clearly differentiated. In contrast, radiology embeddings appear more intermixed, with less visual separation between the models' representation spaces. Nonetheless, the MMD analysis confirms that the observed differences are statistically significant across all modalities. For the aggregated radiology dataset, the observed MMD is 0.0214 (null range: 0.0186–0.0214; $p = 0.005$). For the aggregated microscopy dataset, the observed MMD is 0.0212 (null range: 0.0188–0.0212; $p < 0.001$). For the VLP dataset, the observed MMD is again 0.0214 (null range: 0.0186–0.0214; $p = 0.007$). These results indicate that models trained on subfigure-level data yield significantly different representation spaces compared to those trained on compound figures.

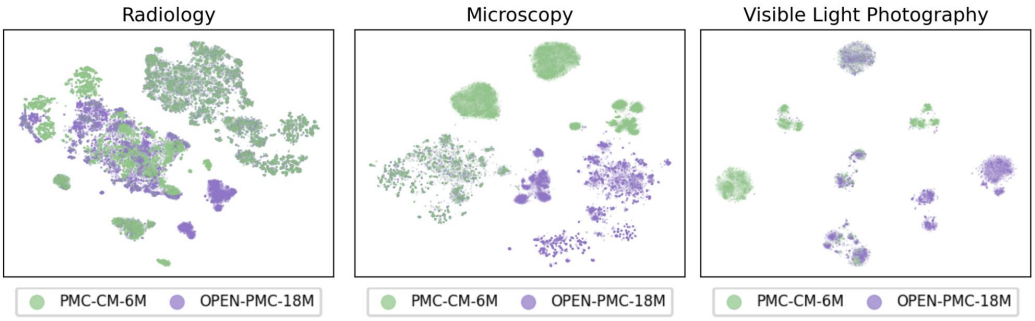

Figure 4: t-SNE visualizations of models embeddings trained on OPEN-PMC-18M and PMC-6M on three imaging modalities, illustrating the structure and separation of the learned representation spaces. MMD analysis reveals statistically significant differences in embedding distributions across all imaging modalities.

5 Limitations and Open Challenges in Biomedical Vision–Language Representation Learning

Our findings suggest that in the context of VLM representation learning, data quality and dataset scale should be viewed as complementary axes in building effective and robust biomedical VLMs. Subfigure extraction, used here as a means to improve alignment quality demonstrates clear benefits, particularly in visually heterogeneous domains such as microscopy and visible light photography, as shown in Figure 2. Radiology, however, exhibits more limited gains. These observations raise the importance of modality-aware pretraining strategies, where both model architectures and data curation pipelines are adapted to the unique characteristics of each imaging modality. While our results highlight promising trends, we note that additional analysis is required, particularly in radiology, across a broader and more diverse set of downstream tasks. Such evaluation will help clarify when and where subfigure extraction yields the greatest benefit. Given the strong performance and robustness of encoders trained on OPEN-PMC-18M, future work includes exploring their integration with large language model decoders for downstream tasks that require generative reasoning over visual inputs, such as medical report generation and visual question answering.

We recognize that scaling and curating large biomedical datasets brings challenges that extend beyond improving model performance. To support transparency and reproducibility, we release all dataset filtering criteria, subfigure detection models, and training pipelines. However, interpretability remains an open challenge in VLMs and particularly in the biomedical domain. Although our models are not intended for clinical deployment, they could be fine-tuned or adapted for various clinical application. However, without rigorous validation and careful consideration of clinical safety, such use poses serious risks. Furthermore, our datasets, sourced from open-access repositories such as PMC, may reflect underlying biases tied to specific institutions, imaging protocols, or publication norms. These factors can influence model behavior in subtle ways, limiting generalizability, especially when applied to underrepresented populations or distinct clinical settings.

6 Conclusion

In this paper we addressed a critical gap in the design of high-fidelity multimodal medical datasets, aiming to advance robust and generalizable representation learning. We evaluated the effectiveness and robustness of subfigure extraction. We introduced OPEN-PMC-18M, one of the largest and highest quality image-caption pairs to date. Models trained on OPEN-PMC-18M consistently outperform existing benchmarks across radiology, microscopy, and visible light photography. These findings lay the groundwork for more generalizable medical VLMs and better aligned with the complex realities of biomedical data.

References

Baghbanzadeh, N., Fallahpour, A., Parhizkar, Y., Ogidi, F., Roy, S., Ashkezari, S., Khazaie, V. R., Colacci, M., Etemad, A., Afkanpour, A., et al. (2025). Advancing medical representation learning through high-quality data. *arXiv preprint arXiv:2503.14377*.

Carion, N., Massa, F., Synnaeve, G., Usunier, N., Kirillov, A., and Zagoruyko, S. (2020). End-to-end object detection with transformers. In *European conference on computer vision*, pages 213–229. Springer.

Dosovitskiy, A., Beyer, L., Kolesnikov, A., Weissenborn, D., Zhai, X., Unterthiner, T., Dehghani, M., Minderer, M., Heigold, G., Gelly, S., et al. (2020). An image is worth 16x16 words: Transformers for image recognition at scale. In *International Conference on Learning Representations*.

García Seco de Herrera, A., Schaer, R., Bromuri, S., and Müller, H. (2016). Overview of the ImageCLEF 2016 medical task. In *Working Notes of CLEF 2016 (Cross Language Evaluation Forum)*.

Girdhar, R., El-Nouby, A., Liu, Z., Singh, M., Alwala, K. V., Joulin, A., and Misra, I. (2023). Imagebind: One embedding space to bind them all. In *Proceedings of the IEEE/CVF Conference on Computer Vision and Pattern Recognition*, pages 15180–15190.

Gretton, A., Borgwardt, K. M., Rasch, M. J., Schölkopf, B., and Smola, A. (2012). A kernel two-sample test. *The Journal of Machine Learning Research*, 13(1):723–773.

Gu, Y., Tinn, R., Cheng, H., Lucas, M., Usuyama, N., Liu, X., Naumann, T., Gao, J., and Poon, H. (2020). Domain-specific language model pretraining for biomedical natural language processing.

Huang, J.-H., Yang, C.-H. H., Liu, F., Tian, M., Liu, Y.-C., Wu, T.-W., Lin, I., Wang, K., Morikawa, H., Chang, H., et al. (2021). Deepopht: medical report generation for retinal images via deep models and visual explanation. In *Proceedings of the IEEE/CVF winter conference on applications of computer vision*, pages 2442–2452.

Ikezogwo, W., Seyfioglu, S., Ghezloo, F., Geva, D., Sheikh Mohammed, F., Anand, P. K., Krishna, R., and Shapiro, L. (2024). Quilt-1m: One million image-text pairs for histopathology. *Advances in Neural Information Processing Systems*, 36.

Jia, C., Yang, Y., Xia, Y., Chen, Y.-T., Parekh, Z., Pham, H., Le, Q., Sung, Y.-H., Li, Z., and Duerig, T. (2021). Scaling up visual and vision-language representation learning with noisy text supervision. In *International conference on machine learning*, pages 4904–4916. PMLR.

Johnson, A. E., Pollard, T. J., Berkowitz, S. J., Greenbaum, N. R., Lungren, M. P., Deng, C.-y., Mark, R. G., and Horng, S. (2019). Mimic-cxr, a de-identified publicly available database of chest radiographs with free-text reports. *Scientific data*, 6(1):317.

Kalpathy-Cramer, J., García Seco de Herrera, A., Demner-Fushman, D., Antani, S., Bedrick, S., and Müller, H. (2014). Evaluating performance of biomedical image retrieval systems– an overview of the medical image retrieval task at ImageCLEF 2004–2014. *Computerized Medical Imaging and Graphics*.

Lin, W., Zhao, Z., Zhang, X., Wu, C., Zhang, Y., Wang, Y., and Xie, W. (2023a). Pmc-clip: Contrastive language-image pre-training using biomedical documents. In *International Conference on Medical Image Computing and Computer-Assisted Intervention*, pages 525–536. Springer.

Lin, Z., Zhang, D., Tao, Q., Shi, D., Haffari, G., Wu, Q., He, M., and Ge, Z. (2023b). Medical visual question answering: A survey. *Artificial Intelligence in Medicine*, page 102611.

Liu, S., Li, F., Zhang, H., Yang, X., Qi, X., Su, H., Zhu, J., and Zhang, L. (2022). DAB-DETR: Dynamic anchor boxes are better queries for DETR. In *International Conference on Learning Representations*.

Liu, X., Li, W., and Yuan, Y. (2024). Diffrect: Latent diffusion label rectification for semi-supervised medical image segmentation. In *International Conference on Medical Image Computing and Computer-Assisted Intervention*, pages 56–66. Springer.

Lozano, A., Sun, M. W., Burgess, J., Chen, L., Nirschl, J. J., Gu, J., Lopez, I., Aklilu, J., Katzer, A. W., Chiu, C., et al. (2025). Biomedica: An open biomedical image-caption archive, dataset, and vision-language models derived from scientific literature. *arXiv preprint arXiv:2501.07171*.

Methani, N., Ganguly, P., Khapra, M. M., and Kumar, P. (2020). Plotqa: Reasoning over scientific plots. In *The IEEE Winter Conference on Applications of Computer Vision (WACV)*.

Oord, A. v. d., Li, Y., and Vinyals, O. (2018). Representation learning with contrastive predictive coding. *arXiv preprint arXiv:1807.03748*.

Pacheco, A. G., Lima, G. R., Salomao, A. S., Krohling, B., Biral, I. P., de Angelo, G. G., Alves Jr, F. C., Esgario, J. G., Simora, A. C., Castro, P. B., et al. (2020). Pad-ufes-20: A skin lesion dataset composed of patient data and clinical images collected from smartphones. *Data in brief*, 32:106221.

Pelka, O., Koitka, S., Rückert, J., Nensa, F., and Friedrich, C. M. (2018). Radiology objects in context (roco): a multimodal image dataset. In *Intravascular Imaging and Computer Assisted Stenting and Large-Scale Annotation of Biomedical Data and Expert Label Synthesis: 7th Joint International Workshop, CVII-STENT 2018 and Third International Workshop, LABELS 2018, Held in Conjunction with MICCAI 2018, Granada, Spain, September 16, 2018, Proceedings 3*, pages 180–189. Springer.

Radford, A., Kim, J. W., Hallacy, C., Ramesh, A., Goh, G., Agarwal, S., Sastry, G., Askell, A., Mishkin, P., Clark, J., et al. (2021). Learning transferable visual models from natural language supervision. In *International conference on machine learning*, pages 8748–8763. PMLR.

Subramanian, S., Wang, L. L., Mehta, S., Bogin, B., van Zuylen, M., Parasa, S., Singh, S., Gardner, M., and Hajishirzi, H. (2020). Medicat: A dataset of medical images, captions, and textual references. *arXiv preprint arXiv:2010.06000*.

Tschandl, P., Rosendahl, C., and Kittler, H. (2018). The ham10000 dataset, a large collection of multi-source dermatoscopic images of common pigmented skin lesions. *Scientific data*, 5(1):1–9.

Tsutsui, S. and Crandall, D. J. (2017). A data driven approach for compound figure separation using convolutional neural networks. In *2017 14th IAPR International Conference on Document Analysis and Recognition (ICDAR)*, volume 1, pages 533–540. IEEE.

Wilcoxon, F. (1945). Individual comparisons by ranking methods. *Biometrics Bulletin*, 1(6):80–83.

Yang, J., Shi, R., and Ni, B. (2021). Medmnist classification decathlon: A lightweight automl benchmark for medical image analysis. In *IEEE 18th International Symposium on Biomedical Imaging (ISBI)*, pages 191–195.

Yang, J., Shi, R., Wei, D., Liu, Z., Zhao, L., Ke, B., Pfister, H., and Ni, B. (2023). Medmnist v2-a large-scale lightweight benchmark for 2d and 3d biomedical image classification. *Scientific Data*, 10(1):41.

Yao, T., Qu, C., Liu, Q., Deng, R., Tian, Y., Xu, J., Jha, A., Bao, S., Zhao, M., Fogo, A. B., et al. (2021). Compound figure separation of biomedical images with side loss. In *Deep Generative Models, and Data Augmentation, Labelling, and Imperfections: First Workshop, DGM4MICCAI 2021, and First Workshop, DALI 2021, Held in Conjunction with MICCAI 2021, Strasbourg, France, October 1, 2021, Proceedings 1*, pages 173–183. Springer.

Zhang, S., Xu, Y., Usuyama, N., Xu, H., Bagga, J., Tinn, R., Preston, S., Rao, R., Wei, M., Valluri, N., et al. (2023). Biomedclip: a multimodal biomedical foundation model pretrained from fifteen million scientific image-text pairs. *arXiv preprint arXiv:2303.00915*.

Ángel E. Esteban, López-Pérez, M., Colomer, A., Sales, M. A., Molina, R., and Naranjo, V. (2019). A new optical density granulometry-based descriptor for the classification of prostate histological images using shallow and deep gaussian processes. *Computer Methods and Programs in Biomedicine*, 178:303–317.

NeurIPS Paper Checklist

1. **Claims**

   Question: Do the main claims made in the abstract and introduction accurately reflect the paper's contributions and scope?

   Answer: [Yes]

   Justification: The main claims in the abstract and introduction are well-aligned with the paper's actual contributions. They emphasize the creation of a high-quality biomedical vision-language dataset and its impact on representation learning, which is thoroughly supported by the methodology, experiments, and evaluations presented in the paper.

   Guidelines:

   - The answer NA means that the abstract and introduction do not include the claims made in the paper.
   - The abstract and/or introduction should clearly state the claims made, including the contributions made in the paper and important assumptions and limitations. A No or NA answer to this question will not be perceived well by the reviewers.
   - The claims made should match theoretical and experimental results, and reflect how much the results can be expected to generalize to other settings.
   - It is fine to include aspirational goals as motivation as long as it is clear that these goals are not attained by the paper.

2. **Limitations**

   Question: Does the paper discuss the limitations of the work performed by the authors?

   Answer: [Yes]

   Justification: We include a "Insights, Limitations, and Broader Considerations" section where we discuss the current limitations of our approach and outline potential directions to address them in future research.

   Guidelines:

   - The answer NA means that the paper has no limitation while the answer No means that the paper has limitations, but those are not discussed in the paper.
   - The authors are encouraged to create a separate "Limitations" section in their paper.
   - The paper should point out any strong assumptions and how robust the results are to violations of these assumptions (e.g., independence assumptions, noiseless settings, model well-specification, asymptotic approximations only holding locally). The authors should reflect on how these assumptions might be violated in practice and what the implications would be.
   - The authors should reflect on the scope of the claims made, e.g., if the approach was only tested on a few datasets or with a few runs. In general, empirical results often depend on implicit assumptions, which should be articulated.
   - The authors should reflect on the factors that influence the performance of the approach. For example, a facial recognition algorithm may perform poorly when image resolution is low or images are taken in low lighting. Or a speech-to-text system might not be used reliably to provide closed captions for online lectures because it fails to handle technical jargon.
   - The authors should discuss the computational efficiency of the proposed algorithms and how they scale with dataset size.
   - If applicable, the authors should discuss possible limitations of their approach to address problems of privacy and fairness.
   - While the authors might fear that complete honesty about limitations might be used by reviewers as grounds for rejection, a worse outcome might be that reviewers discover limitations that aren't acknowledged in the paper. The authors should use their best judgment and recognize that individual actions in favor of transparency play an important role in developing norms that preserve the integrity of the community. Reviewers will be specifically instructed to not penalize honesty concerning limitations.

3. **Theory Assumptions and Proofs**

Question: For each theoretical result, does the paper provide the full set of assumptions and a complete (and correct) proof?

Answer: [NA]

Justification: We do not have any theoretical results.

Guidelines:

- The answer NA means that the paper does not include theoretical results.
- All the theorems, formulas, and proofs in the paper should be numbered and cross-referenced.
- All assumptions should be clearly stated or referenced in the statement of any theorems.
- The proofs can either appear in the main paper or the supplemental material, but if they appear in the supplemental material, the authors are encouraged to provide a short proof sketch to provide intuition.
- Inversely, any informal proof provided in the core of the paper should be complemented by formal proofs provided in appendix or supplemental material.
- Theorems and Lemmas that the proof relies upon should be properly referenced.

4. **Experimental Result Reproducibility**

Question: Does the paper fully disclose all the information needed to reproduce the main experimental results of the paper to the extent that it affects the main claims and/or conclusions of the paper (regardless of whether the code and data are provided or not)?

Answer: [Yes]

Justification: We provide all the details of our model training and evaluation pipeline.

Guidelines:

- The answer NA means that the paper does not include experiments.
- If the paper includes experiments, a No answer to this question will not be perceived well by the reviewers: Making the paper reproducible is important, regardless of whether the code and data are provided or not.
- If the contribution is a dataset and/or model, the authors should describe the steps taken to make their results reproducible or verifiable.
- Depending on the contribution, reproducibility can be accomplished in various ways. For example, if the contribution is a novel architecture, describing the architecture fully might suffice, or if the contribution is a specific model and empirical evaluation, it may be necessary to either make it possible for others to replicate the model with the same dataset, or provide access to the model. In general. releasing code and data is often one good way to accomplish this, but reproducibility can also be provided via detailed instructions for how to replicate the results, access to a hosted model (e.g., in the case of a large language model), releasing of a model checkpoint, or other means that are appropriate to the research performed.
- While NeurIPS does not require releasing code, the conference does require all submissions to provide some reasonable avenue for reproducibility, which may depend on the nature of the contribution. For example
  (a) If the contribution is primarily a new algorithm, the paper should make it clear how to reproduce that algorithm.
  (b) If the contribution is primarily a new model architecture, the paper should describe the architecture clearly and fully.
  (c) If the contribution is a new model (e.g., a large language model), then there should either be a way to access this model for reproducing the results or a way to reproduce the model (e.g., with an open-source dataset or instructions for how to construct the dataset).
  (d) We recognize that reproducibility may be tricky in some cases, in which case authors are welcome to describe the particular way they provide for reproducibility. In the case of closed-source models, it may be that access to the model is limited in some way (e.g., to registered users), but it should be possible for other researchers to have some path to reproducing or verifying the results.

5. **Open access to data and code**

   Question: Does the paper provide open access to the data and code, with sufficient instructions to faithfully reproduce the main experimental results, as described in supplemental material?

   Answer: [Yes]

   Justification: To facilitate reproducibility and support further research, we have made our codebase, pretrained model weights, and the dataset publicly available through our GitHub and Hugging Face repositories. Each repository includes comprehensive documentation and usage instructions to enable easy adoption and integration by the research community.

   Guidelines:

   - The answer NA means that paper does not include experiments requiring code.
   - Please see the NeurIPS code and data submission guidelines (`https://nips.cc/public/guides/CodeSubmissionPolicy`) for more details.
   - While we encourage the release of code and data, we understand that this might not be possible, so "No" is an acceptable answer. Papers cannot be rejected simply for not including code, unless this is central to the contribution (e.g., for a new open-source benchmark).
   - The instructions should contain the exact command and environment needed to run to reproduce the results. See the NeurIPS code and data submission guidelines (`https://nips.cc/public/guides/CodeSubmissionPolicy`) for more details.
   - The authors should provide instructions on data access and preparation, including how to access the raw data, preprocessed data, intermediate data, and generated data, etc.
   - The authors should provide scripts to reproduce all experimental results for the new proposed method and baselines. If only a subset of experiments are reproducible, they should state which ones are omitted from the script and why.
   - At submission time, to preserve anonymity, the authors should release anonymized versions (if applicable).
   - Providing as much information as possible in supplemental material (appended to the paper) is recommended, but including URLs to data and code is permitted.

6. **Experimental Setting/Details**

   Question: Does the paper specify all the training and test details (e.g., data splits, hyperparameters, how they were chosen, type of optimizer, etc.) necessary to understand the results?

   Answer: [Yes]

   Justification: Yes. The paper provides comprehensive training and evaluation details.

   Guidelines:

   - The answer NA means that the paper does not include experiments.
   - The experimental setting should be presented in the core of the paper to a level of detail that is necessary to appreciate the results and make sense of them.
   - The full details can be provided either with the code, in appendix, or as supplemental material.

7. **Experiment Statistical Significance**

   Question: Does the paper report error bars suitably and correctly defined or other appropriate information about the statistical significance of the experiments?

   Answer: [Yes]

   Justification: The paper reports performance metrics across multiple runs and includes standard deviations to indicate variability, providing a clear understanding of the statistical significance and robustness of the results.

   Guidelines:

   - The answer NA means that the paper does not include experiments.

- The authors should answer "Yes" if the results are accompanied by error bars, confidence intervals, or statistical significance tests, at least for the experiments that support the main claims of the paper.
- The factors of variability that the error bars are capturing should be clearly stated (for example, train/test split, initialization, random drawing of some parameter, or overall run with given experimental conditions).
- The method for calculating the error bars should be explained (closed form formula, call to a library function, bootstrap, etc.)
- The assumptions made should be given (e.g., Normally distributed errors).
- It should be clear whether the error bar is the standard deviation or the standard error of the mean.
- It is OK to report 1-sigma error bars, but one should state it. The authors should preferably report a 2-sigma error bar than state that they have a 96% CI, if the hypothesis of Normality of errors is not verified.
- For asymmetric distributions, the authors should be careful not to show in tables or figures symmetric error bars that would yield results that are out of range (e.g. negative error rates).
- If error bars are reported in tables or plots, The authors should explain in the text how they were calculated and reference the corresponding figures or tables in the text.

8. **Experiments Compute Resources**

   Question: For each experiment, does the paper provide sufficient information on the computer resources (type of compute workers, memory, time of execution) needed to reproduce the experiments?

   Answer: [Yes]

   Justification: We report the total training time of our models along with details of the GPU used.

   Guidelines:

   - The answer NA means that the paper does not include experiments.
   - The paper should indicate the type of compute workers CPU or GPU, internal cluster, or cloud provider, including relevant memory and storage.
   - The paper should provide the amount of compute required for each of the individual experimental runs as well as estimate the total compute.
   - The paper should disclose whether the full research project required more compute than the experiments reported in the paper (e.g., preliminary or failed experiments that didn't make it into the paper).

9. **Code Of Ethics**

   Question: Does the research conducted in the paper conform, in every respect, with the NeurIPS Code of Ethics `https://neurips.cc/public/EthicsGuidelines`?

   Answer: [Yes]

   Justification: The research complies with the NeurIPS Code of Ethics by using publicly available data, providing open-source code, and clearly stating that the models are for research use only.

   Guidelines:

   - The answer NA means that the authors have not reviewed the NeurIPS Code of Ethics.
   - If the authors answer No, they should explain the special circumstances that require a deviation from the Code of Ethics.
   - The authors should make sure to preserve anonymity (e.g., if there is a special consideration due to laws or regulations in their jurisdiction).

10. **Broader Impacts**

    Question: Does the paper discuss both potential positive societal impacts and negative societal impacts of the work performed?

    Answer: [Yes]

Justification: It is discussed in section "Insights, Limitations, and Broader Considerations"

Guidelines:

- The answer NA means that there is no societal impact of the work performed.
- If the authors answer NA or No, they should explain why their work has no societal impact or why the paper does not address societal impact.
- Examples of negative societal impacts include potential malicious or unintended uses (e.g., disinformation, generating fake profiles, surveillance), fairness considerations (e.g., deployment of technologies that could make decisions that unfairly impact specific groups), privacy considerations, and security considerations.
- The conference expects that many papers will be foundational research and not tied to particular applications, let alone deployments. However, if there is a direct path to any negative applications, the authors should point it out. For example, it is legitimate to point out that an improvement in the quality of generative models could be used to generate deepfakes for disinformation. On the other hand, it is not needed to point out that a generic algorithm for optimizing neural networks could enable people to train models that generate Deepfakes faster.
- The authors should consider possible harms that could arise when the technology is being used as intended and functioning correctly, harms that could arise when the technology is being used as intended but gives incorrect results, and harms following from (intentional or unintentional) misuse of the technology.
- If there are negative societal impacts, the authors could also discuss possible mitigation strategies (e.g., gated release of models, providing defenses in addition to attacks, mechanisms for monitoring misuse, mechanisms to monitor how a system learns from feedback over time, improving the efficiency and accessibility of ML).

11. **Safeguards**

Question: Does the paper describe safeguards that have been put in place for responsible release of data or models that have a high risk for misuse (e.g., pretrained language models, image generators, or scraped datasets)?

Answer: [Yes]

Justification: The paper includes clear disclaimers stating that the models are intended solely for research use and not for clinical deployment. Additionally, all data used in the curation process are sourced from publicly available resource, ensuring that no private or sensitive information is exposed.

Guidelines:

- The answer NA means that the paper poses no such risks.
- Released models that have a high risk for misuse or dual-use should be released with necessary safeguards to allow for controlled use of the model, for example by requiring that users adhere to usage guidelines or restrictions to access the model or implementing safety filters.
- Datasets that have been scraped from the Internet could pose safety risks. The authors should describe how they avoided releasing unsafe images.
- We recognize that providing effective safeguards is challenging, and many papers do not require this, but we encourage authors to take this into account and make a best faith effort.

12. **Licenses for existing assets**

Question: Are the creators or original owners of assets (e.g., code, data, models), used in the paper, properly credited and are the license and terms of use explicitly mentioned and properly respected?

Answer: [Yes]

Justification: All external assets used in the paper, including datasets, models, and code, are properly credited with citations.

Guidelines:

- The answer NA means that the paper does not use existing assets.

- The authors should cite the original paper that produced the code package or dataset.
- The authors should state which version of the asset is used and, if possible, include a URL.
- The name of the license (e.g., CC-BY 4.0) should be included for each asset.
- For scraped data from a particular source (e.g., website), the copyright and terms of service of that source should be provided.
- If assets are released, the license, copyright information, and terms of use in the package should be provided. For popular datasets, `paperswithcode.com/datasets` has curated licenses for some datasets. Their licensing guide can help determine the license of a dataset.
- For existing datasets that are re-packaged, both the original license and the license of the derived asset (if it has changed) should be provided.
- If this information is not available online, the authors are encouraged to reach out to the asset's creators.

13. **New Assets**

    Question: Are new assets introduced in the paper well documented and is the documentation provided alongside the assets?

    Answer: [Yes]

    Justification: All new assets introduced in the paper, including the OPEN-PMC-18M dataset and pretrained models, are thoroughly documented. The documentation is provided alongside the assets in the public repositories to ensure ease of use and reproducibility.

    Guidelines:

    - The answer NA means that the paper does not release new assets.
    - Researchers should communicate the details of the dataset/code/model as part of their submissions via structured templates. This includes details about training, license, limitations, etc.
    - The paper should discuss whether and how consent was obtained from people whose asset is used.
    - At submission time, remember to anonymize your assets (if applicable). You can either create an anonymized URL or include an anonymized zip file.

14. **Crowdsourcing and Research with Human Subjects**

    Question: For crowdsourcing experiments and research with human subjects, does the paper include the full text of instructions given to participants and screenshots, if applicable, as well as details about compensation (if any)?

    Answer: [NA]

    Justification: We do not have any human subjects.

    Guidelines:

    - The answer NA means that the paper does not involve crowdsourcing nor research with human subjects.
    - Including this information in the supplemental material is fine, but if the main contribution of the paper involves human subjects, then as much detail as possible should be included in the main paper.
    - According to the NeurIPS Code of Ethics, workers involved in data collection, curation, or other labor should be paid at least the minimum wage in the country of the data collector.

15. **Institutional Review Board (IRB) Approvals or Equivalent for Research with Human Subjects**

    Question: Does the paper describe potential risks incurred by study participants, whether such risks were disclosed to the subjects, and whether Institutional Review Board (IRB) approvals (or an equivalent approval/review based on the requirements of your country or institution) were obtained?

    Answer: [NA]

Justification: The study does not involve human subjects or private individual data. All data used are sourced from publicly available open-access articles, and no identifiable personal information is included, so IRB approval was not required.

Guidelines:

- The answer NA means that the paper does not involve crowdsourcing nor research with human subjects.
- Depending on the country in which research is conducted, IRB approval (or equivalent) may be required for any human subjects research. If you obtained IRB approval, you should clearly state this in the paper.
- We recognize that the procedures for this may vary significantly between institutions and locations, and we expect authors to adhere to the NeurIPS Code of Ethics and the guidelines for their institution.
- For initial submissions, do not include any information that would break anonymity (if applicable), such as the institution conducting the review.